Genes and enzymes involved in the biodegradation of the quaternary carbon compound pivalate in the denitrifying Thauera humireducens strain PIV -1

Christian Jacoby, Christa Ebenau-Jehle, Katharina Saum, Nico Jehmlich, Martin von Bergen, Thomas Brüls, Matthias Boll

environmental microbiology

Environmental Microbiology (2022) **24**(7), 3181–3194 doi:10.1111/1462-2920.16021

Genes and enzymes involved in the biodegradation of the quaternary carbon compound pivalate in the denitrifying *Thauera humireducens* strain PIV-1

Christian Jacoby,[1] Christa Ebenau-Jehle,[1] Katharina Saum,[1] Nico Jehmlich,[2,3] Martin von Bergen,[2,3,4] Thomas Brüls[5] and Matthias Boll[1*]

[1]*Faculty of Biology - Microbiology, University of Freiburg, Freiburg, 79104, Germany.*

[2]*Department of Analytical Chemistry, Helmholtz Centre for Environmental Research - UFZ, Leipzig, 04318, Germany.*

[3]*Department of Molecular Systems Biology, Helmholtz, Centre for Environmental Research - UFZ, Leipzig, 04318, Germany.*

[4]*Faculty of Life Sciences, Institute of Biochemistry, University of Leipzig, Brüderstr. 34, Leipzig, 04103, Germany.*

[5]*Génomique Métabolique, Genoscope, Institut François Jacob, CEA, CNRS, Univ Evry, Université Paris-Saclay, Evry, France.*

Summary

Quaternary carbon-containing compounds exist in natural and fossil oil-derived products and are used in chemical and pharmaceutical applications up to industrial scale. Due to the inaccessibility of the quaternary carbon atom for a direct oxidative or reductive attack, they are considered as persistent in the environment. Here, we investigated the unknown degradation of the quaternary carbon-containing model compound pivalate (2,2-dimethyl-propionate) in the denitrifying bacterium *Thauera humireducens* strain PIV-1 (formerly *Thauera pivalivorans*). We provide multiple evidence for a pathway comprising the activation to pivalyl-CoA and the carbon skeleton rearrangement to isovaleryl-CoA. Subsequent reactions proceed similar to the catabolic leucine degradation pathway such as the carboxylation to 3-methylglutaconyl-CoA and the cleavage of 3-methyl-3-hydroxyglutaryl-CoA to acetyl-CoA and acetoacetate. The completed genome of *Thauera humireducens* strain PIV-1 together with proteomic data was used to identify pivalate-upregulated gene clusters including genes putatively encoding pivalate CoA ligase and adenosylcobalamin-dependent pivalyl-CoA mutase. A pivalate-induced gene encoding a putative carboxylic acid CoA ligase was heterologously expressed, and its highly enriched product exhibited pivalate CoA ligase activity. The results provide the first experimental insights into the biodegradation pathway of a quaternary carbon-containing model compound that serves as a blueprint for the degradation of related quaternary carbon-containing compounds.

Introduction

Quaternary carbon containing moieties have been identified in a number of natural products (Dembitsky, 2006; Bisel *et al*., 2008). The neopentyl (2,2-dimethylpropyl) group, the minimal structural moiety with a quaternary carbon atom, is found in ginkgolides, sterols with highly branched side chains from marine sponges or higher plants, or peptides containing either of the two enantiomers of the non-proteinogenic amino acid *tert*-leucine (Bisel *et al*., 2008), e.g. in bottromycins, a class of macrocyclic peptides with antibiotic activity (Franz *et al*., 2021). The identification of branched alkanes with quaternary substituted carbon atoms of biological origin in modern and ancient geologic samples supports their wide distribution in nature (Kenig *et al*., 2003). The neopentyl group is also found in many fossil-oil derived branched hydrocarbons including the gasoline isooctane, and the synthetic neopentyl glycol (2,2-dimethyl-1,3-propanediol) that is widely used for the synthesis of polyesters, plasticizers, lubricants, pharmaceuticals and resins. Esters of the neopentyl group containing pivalic acid (2,2-dimethyl-propionic acid) are frequently used in prodrugs to increase their bioavailability (Brass, 2002). After hydrolysis from the prodrug, the pivalate formed is excreted as pivaloylcarnitine conjugate, which contributes significantly to the release of pivalate to the environment.

Received 21 March, 2022; revised 14 April, 2022; accepted 17 April, 2022. *For correspondence. E-mail matthias.boll@biologie.uni-freiburg.de; Tel. +49 761 2032649; Fax +49 761 2032626.

The biodegradation of compounds containing a quaternary carbon is challenging due to its inaccessibility for a direct oxidative or reductive attack. For this reason, the few known examples of degradation pathways in aerobic microorganisms often proceed via activation of the carbon atom in α-position to the quaternary one (summarized in Kniemeyer *et al*., 1999). In camphor or eucalyptol, this position already contains a ketone functionality, which enables the oxidation to a lactone via a Baeyer–Villiger oxygenase followed by the hydrolysis to a tertiary alcohol (Trudgill, 1994; Marmulla and Harder, 2014). During the aerobic degradation of steroids with quaternary compounds, such as cholesterol, a methyl group in α-position of a quaternary carbon (C10) is stepwise oxidized by a cytochrome P450 monooxygenase to an aldehyde, which is finally oxidatively released as formate (Shyadehi *et al*., 1996), similar to the well-known reaction of aromatase that converts androgens to estrogens (Simpson *et al*., 2002). These examples exemplify that the degradation of quaternary carbon-containing compounds in aerobic microorganisms depends on oxygenases.

Under anoxic conditions, the current knowledge of quaternary carbon compound degradation pathways is limited to studies with denitrifying bacteria that degrade quaternary carbon-containing steroids such as androgens or cholesterol. During degradation of the latter, the water-dependent hydroxylation of an unactivated primary carbon at the isoprenoid is achieved by an enzyme cascade involving a tertiary alcohol intermediate (Dermer and Fuchs, 2012; Jacoby *et al*., 2018), and its ATP-dependent conversion to an allylic alcohol (Wang *et al*., 2013; Jacoby *et al*., 2020a; Jacoby *et al*., 2021). This cascade allows for the oxygen-independent hydroxylation of an unactivated methyl group next to a tertiary carbon; however, it is not applicable to the quaternary carbons at C10 and C13 of the androstane skeleton (Warnke *et al*., 2017). Interestingly, oestrogen degradation in denitrifying bacteria is initiated by the formation of a quaternary carbon at C10 via S-adenosylmethionine- and methylcobalamin-dependent methylation to androgens (Wang *et al*., 2020; Jacoby *et al*., 2020b). However, this reaction was essentially non-reversible and thus demethylation appears to be no option for the conversion of a quaternary carbon moiety.

Among quaternary carbon-containing compounds, pivalate represents a model compound for studying the biodegradation of compounds with a neopentyl functionality. Its biodegradation to CO_2 has so far only been demonstrated for some denitrifying strains including species of the genera *Thauera*, *Zoogloea* and *Herbaspirillum* (Probian *et al*., 2003). It has also been reported as an intermediate during the complete aerobic degradation of more complex quaternary carbon compounds such as isooctane (Solano-Serena *et al*., 2000, 2004). For the aerobic degradation of pivalate, oxidation of one of the methyl groups to an aldehyde and its subsequent oxidative release as formate has been proposed (Solano-Serena *et al*., 2004), similar to what has been shown for the aerobic degradation of cholesterol (Fig. 1A). This pathway is not an option for denitrifying bacteria, and two alternative pathways have been suggested (Probian *et al*., 2003). The anoxic oxidation of the unactivated methyl group of pivalate to dimethylmalonate is challenging, but may be achieved by addition to fumarate by a glycyl-radical enzyme, similar to what has been shown for n-alkanes (Jarling *et al*., 2012; Wilkes *et al*., 2016) (Fig. 1B). After activation of the alkylsuccinate intermediate to a thioester, a series of β-oxidation steps would finally yield dimethylmalonyl-CoA. The latter may then be decarboxylated to isobutyryl-CoA similar to known malonate decarboxylases (Chohnan and Takamura, 2004). An alternative pathway is initiated by thioesterification to pivalyl-coenzyme A (CoA), followed by carbon skeleton rearrangement to isovaleryl-CoA (3-methylbutyryl-CoA) involving an adenosylcobalamin (AdoCbl, often referred to as coenzyme B12 or simply B12)-dependent pivalyl-CoA mutase (Fig. 1C). Notably, such an activity has already been demonstrated by engineering an isobutyryl-CoA mutase by site-directed mutagenesis and by heterologous expression of a gene encoding a putative AdoCbl-dependent mutase (Kitanishi *et al*., 2015). Isovaleryl-CoA could be further degraded to acetoacetate and acetyl-CoA by enzymes of the common leucine catabolism. There is no experimental evidence for either the aerobic or the two anaerobic degradation pathways of pivalate.

Here, we investigated the unknown degradation pathway of the quaternary carbon-containing model compound pivalate in the denitrifying, pivalate-degrading *Thauera humireducens* strain PIV-1 [*T. humireducens*, previously *Thauera pivalivorans* strain PIV1 (Probian *et al*., 2003)]. We combined *in vitro* assays in extracts from cells grown with pivalate/nitrate with a proteogenomic approach. In addition, the enzyme that initiates anaerobic pivalate degradation was heterologously produced and characterized. The results are in line with a pathway involving an AdoCbl-dependent carbon skeleton rearrangement of the pivalyl-CoA intermediate.

Results and discussion

Large-scale cultivation of T. humireducens *with pivalate and nitrate*

Among the reported denitrifying bacteria growing with pivalate and nitrate as the sole carbon and energy source (Probian *et al*., 2003), *Thauera pivalivorans*, now reclassified as *T. humireducens* (based on the genome

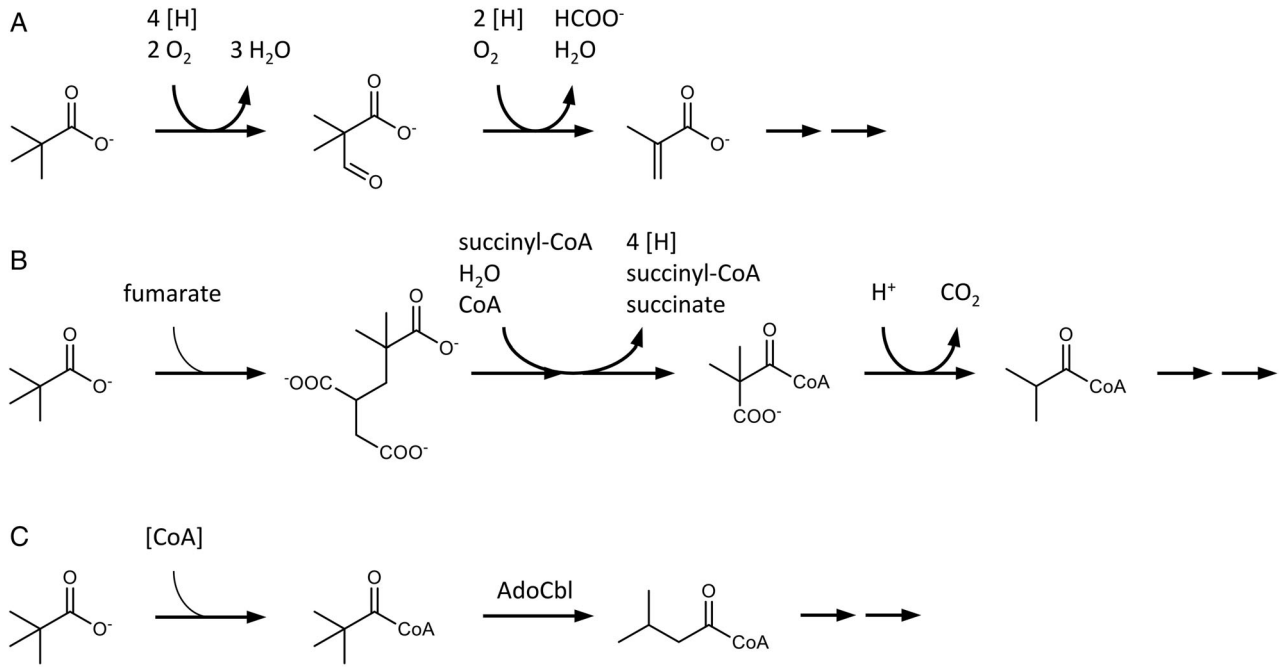

Fig. 1. Putative oxygen-dependent/independent degradation pathways of pivalate.
A. Oxidation of a methyl group to an aldehyde followed by oxidative formate release catalysed by a cytochrome P450 monooxygenase.
B. Anoxic oxidation of a methyl group to dimethylmalonate involving a glycyl radical alkylsuccinyl-CoA synthase and a series of β-oxidation like reactions, followed by decarboxylation.
C. Activation of pivalate to pivalyl-CoA, followed by carbon skeleton rearrangement catalysed by an AdoCbl-dependent mutase. [CoA]: thioesterification variable CoA ester forming enzyme such as ATP-dependent CoA ligases or CoA transferases.

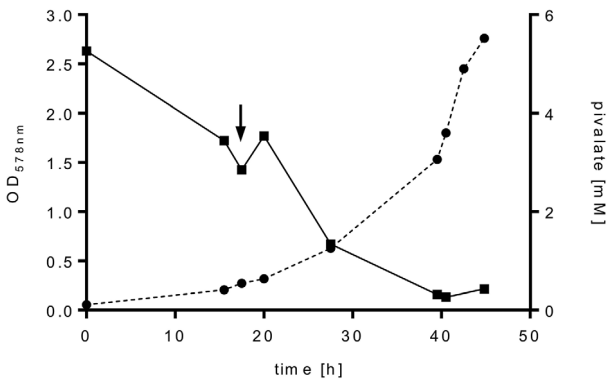

Fig. 2. Large-scale cultivation of *T. humireducens* in a 200-L-fermenter with pivalate/nitrate (3:1). ● OD_{578}, ■ pivalate. The arrow indicates the start of the fed-batch cultivation.

sequence, see below) showed the best growth in terms of doubling time and maximal cell density reached. To obtain biomass sufficient for the planned studies, *T. humireducens* was grown in a 200-L-fermenter using a mineral salt medium supplemented with 5 mM pivalate and 15 mM nitrate (Fig. 2). Close to consumption, pivalate and nitrate were continuously fed using a computer-controlled pump that correlated the pump rate to the growth parameters. Using this fed-batch setup, the doubling time was 8.7 h. Cells were harvested at an optical density of $OD_{578} = 3.0$ yielding 364 g cells (wet mass). This lower than theoretically expected yield (>500 g) can be explained by the strong sedimentation tendency of *T. humireducens*, which resulted in some loss of biomass during the harvest.

Whole-cell CoA-ester pool analyses

To obtain initial insights into the pivalate degradation pathway in *T. humireducens*, CoA esters were extracted from whole cells growing in exponential phase on pivalate and nitrate, and analysed by ultra-performance liquid chromatography (UPLC) coupled to detection by electrospray ionization quadrupole time-of-flight mass spectrometry (ESI-Q-TOF-MS). During these analyses, we focused on characteristic CoA ester intermediates of initial enzymatic steps of the degradation pathway. Pivalyl-CoA, isovaleryl-CoA and 3-methylcrotonyl-CoA were identified as major CoA ester compounds (Table S1) based on comparisons with *m/z* values and retention times of authentic standards. In contrast, neither pivalylsuccinyl-CoA, dimethylmalonyl-CoA nor isobutyryl-CoA was found. These results are in accordance with the pathway depicted in Fig. 1C, whereas no evidence for the alternative pathway shown in Fig. 1B was obtained.

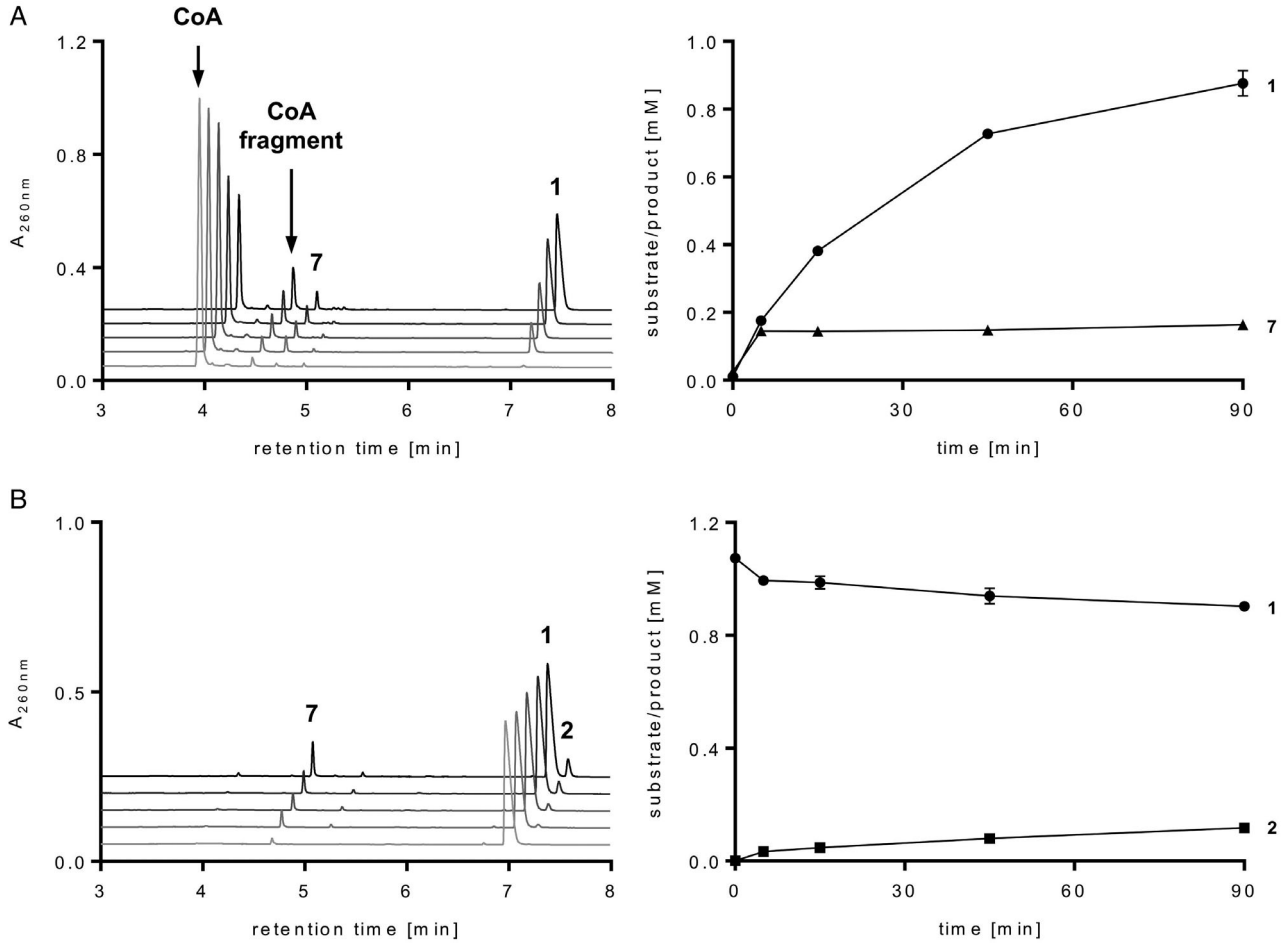

Fig. 3. Time-dependent conversion of pivalate to pivalyl-CoA and isovaleryl-CoA by soluble cell extracts of *T. humireducens*. Left panels, UPLC chromatograms; right panels, time-dependent formation of CoA ester products.
A. Conversion of pivalate to pivalyl-CoA.
B. Conversion of pivalyl-CoA to isovaleryl-CoA. In this assay, enriched pivalate CoA ligase was added to minimize pivalyl-CoA depletion caused by a thioesterase activity. The UPLC-based enzymatic assays contained 2 mg ml^{-1} proteins, samples were taken at 0, 5, 15, 45 and 90 min. (**1**) Pivalyl-CoA, (**2**) isovaleryl-CoA, (**7**) acetyl-CoA. The numbers refer to components identified by ESI-Q-TOF-MS analyses listed in Table S2, and to metabolites depicted in Fig. 5. The error bars refer to the standard deviation of three independent replicates.

In vitro *enzyme assays*

For measurement of a potential ATP-dependent pivalate CoA ligase in extracts of cells grown with pivalate and nitrate, we followed the formation of CoA ester products by UPLC analysis. In our enzymatic assays, we observed the pivalate-, MgATP-, CoA-, cell extract- and time-dependent formation of pivalyl-CoA with a specific activity of 23.1 $\pm$ 1.1 nmol min^{-1} mg^{-1} (Fig. 3A). Pivalyl-CoA (**1**) was identified by its *m/z* value after ESI-Q-TOF-MS/MS analysis and by co-elution with an authentic pivalyl-CoA standard (Table S2). In these assays, the time-dependent formation of additional minor peaks was detected, one of which was identified as acetyl-CoA (**7**). It derived either from pivalyl-CoA degradation or from an acetate CoA ligase activity providing that acetate was present in the cell extract. Another peak was probably a 3′-dephospho-CoA fragment.

To measure the suggested carbon skeleton rearrangement catalysed by a pivalyl-CoA mutase, *in vitro* assays were conducted with chemically synthesized pivalyl-CoA as substrate. The time and cell extract dependent conversion to isovaleryl-CoA was observed at a rate of 5.8 $\pm$ 1.0 nmol min^{-1} mg^{-1} (Fig. 3B). Due to the known photolability of the AdoCbl-dependent mutases, the reaction was carried out in the dark. Indeed, the pivalyl-CoA mutase activity was abolished by 45 min light exposure (8-watt LED lamp, Fig. +S1). Activity of light-inactivated mutase was restored up to 80% after incubation with 20 μM AdoCbl (Fig. S1). Both findings are in agreement with a light-sensitive, AdoCbl-dependent mutase catalysing the conversion of pivalyl-CoA to isovaleryl-CoA.

To analyse the following steps of the anaerobic pivalate degradation, assays were conducted with chemically synthesized isovaleryl-CoA (**2**) and 5 mM

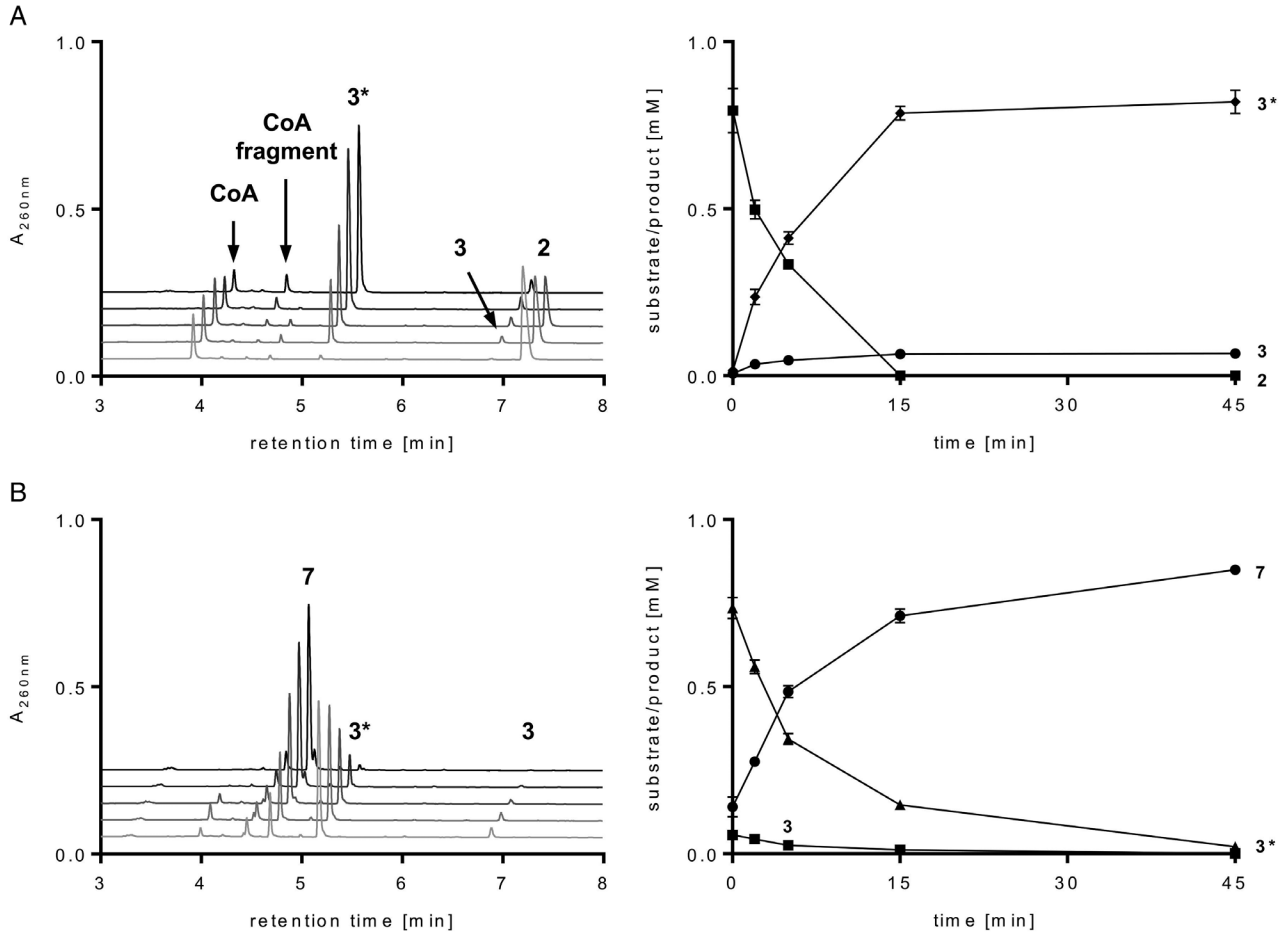

Fig. 4. Time-dependent conversion of isovaleryl-CoA by soluble cell extract of *T. humireducens*. Left panels, UPLC chromatograms; right panels, time-dependent formation of CoA ester products. For chemical structures of detected CoA esters, see Fig. 5.
A. Conversion of isovaleryl-CoA (**2**) to 3-methylcrotonyl-CoA (**3**) and 3-hydroxy-3-methylbutyryl-CoA (**3***) with $K_3[Fe(CN)_6]$ as electron acceptor.
B. Conversion of a mixture of **3** and **3*** (obtained after pre-incubation of isovaleryl-CoA with $K_3[Fe(CN)_6]$ for 30 min) in the presence of 10 mM $NaHCO_3$ and 2 mM MgATP. The UPLC-based enzymatic assays were performed with cell extract containing 2 mg ml^{-1} protein and stopped after 0, 2, 5, 15 and 45 min. (**7**) acetyl-CoA. The error bars refer to the standard deviation of three independent replicates.

ferricyanide ($K_3[Fe(CN)_6]$) as artificial electron acceptors (Fig. 4A). In these assays, the time-dependent consumption of (**2**) was accompanied by the formation of compounds (**3**) and (**3***), which were identified as 3-methylcrotonyl-CoA (**3**) and 3-hydroxy-3-methylbutyryl-CoA (**3***) by ESI-QTOF-MS/MS analyses respectively (Table S2). The conversion of (**3**) to (**3***) at an approximately 1:9 ratio can be explained by an non-specific reaction of a crotonase-like enoyl-CoA hydratase. The 3-methylcrotonyl-CoA (**3**) formed is an intermediate of leucine catabolism and is usually carboxylated to 3-methylglutaconyl-CoA by an ATP- and biotin-dependent enzyme (Massey *et al*., 1976) (Fig. S2). To follow such a reaction, we added 2 mM MgATP and 10 mM $NaHCO_3$ to a mixture of (**3**) and (**3***) that was obtained after 30 min pre-incubation of cell extract with isovaleryl-CoA (**2**) in the presence of 5 mM ferricyanide. We observed the time-dependent consumption of (**3**) and (**3***) and the formation of acetyl-CoA (**7**) (Fig. 4B). No such conversion was observed in the absence of MgATP/$NaHCO_3$. The formation of acetyl-CoA can be explained by the carboxylation of 3-methylcrotonyl-CoA to 3-methylglutaconyl-CoA, its immediate hydration by an enoyl-CoA hydratase to 3-hydroxy-3-methylglutaryl-CoA (**5**), followed by retro-aldol cleavage to acetoacetate and acetyl-CoA according to the leucine catabolic pathway (Fig. S2). Notably, CoA and 5′-dephospho-CoA were always formed to some extent by chemical or enzymatic hydrolysis of CoA esters. The acetoacetate intermediate can be activated to acetoacetyl-CoA that is cleaved to two further acetyl-CoA by β-ketothiolase. To confirm such a pathway, we incubated 0.5 mM acetoacetate with cell extracts in the presence of 2 mM MgATP and 1 mM CoA, and observed the rapid formation of acetyl-CoA,

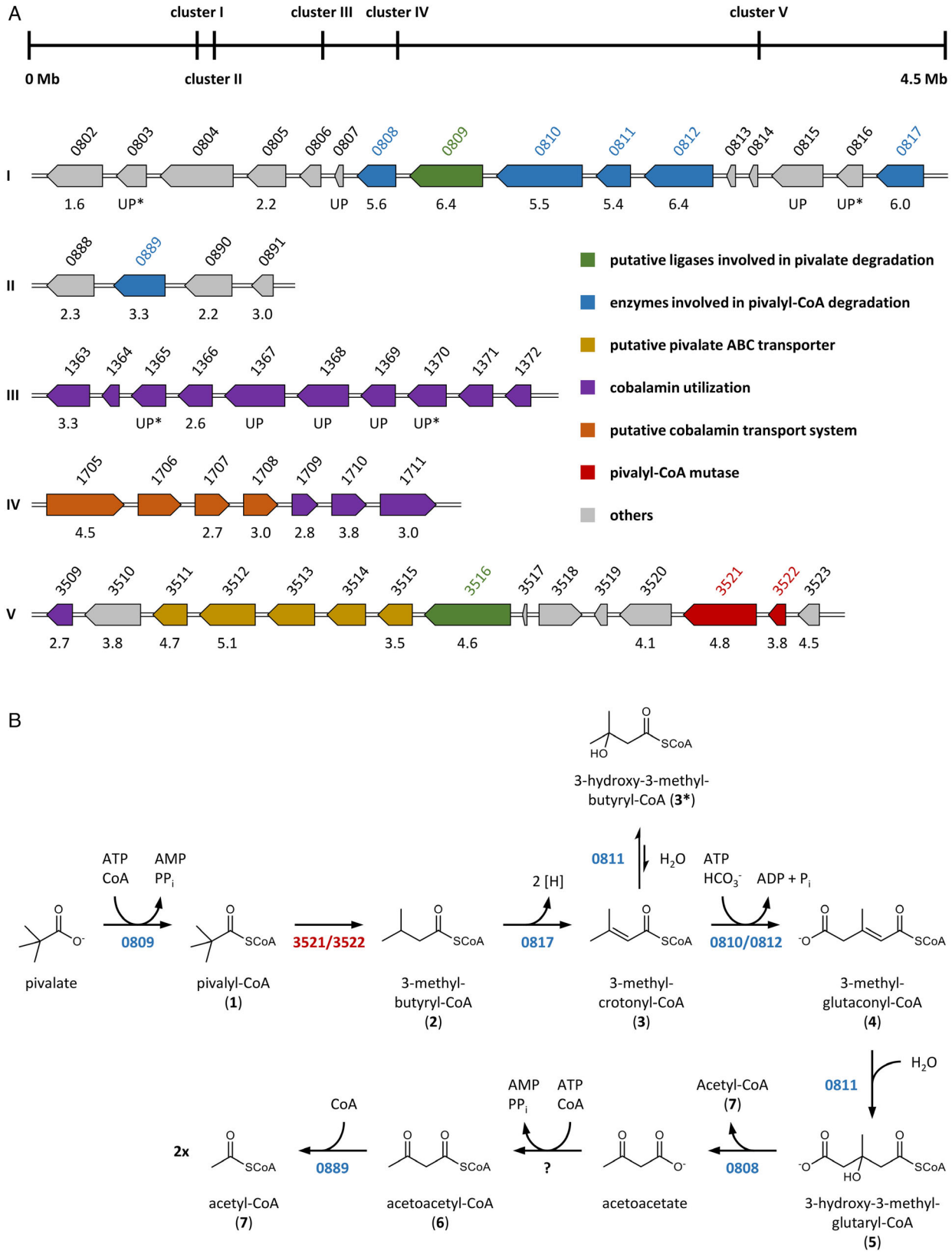

Fig. 5. Legend on next page.

indicating that acetoacetate was activated via a CoA ligase followed by rapid β-ketothiolase catalysed cleavage to two acetyl-CoA (Fig. S3).

In an alternative pathway, the observed 3-hydroxy-3-methylbutyryl-CoA (**3***) intermediate could be directly cleaved to acetoacetyl-CoA and acetone as already reported for leucine catabolism in *Vibrio* species (Nemecek-Marshall *et al*., 1999). To test whether such a pathway is employed during pivalate degradation in *T. humireducens*, we incubated cell extracts with 0.5 mM acetone, 10 mM $NaHCO_3$, 1 mM MgATP and 1 mM CoA. In such assays, no formation of acetoacetyl-CoA/acetyl-CoA was observed. Accordingly, *T. humireducens* did not grow with acetone under denitrifying conditions. Both findings rather rule out that acetone is an intermediate during pivalate degradation.

Complete genome of T. humireducens *strain PIV-1*

In order to identify the key enzymes and their encoding genes, we generated a high-quality genome sequence of *T. humireducens* through a hybrid sequencing approach combining both long and short reads. A single contig corresponding to the main bacterial chromosome was obtained, encompassing 4 498 018 bases (66% GC content) and harbouring 4365 coding sequences, as well as the sequence of a 39 874 base plasmid (60% GC content) containing 34 coding sequences (Fig. S4). Both sequences are available from the ENA/NCBI/DDBJ databases under accession numbers OW011623 and OW011624 (study identifier PRJEB51144). Overall, about 88% of the coding sequences of *T. humireducens* are classified in at least one EGGNOG group (79% into at least one COG group), and its closest sequenced organisms in terms of genome-level gene syntenies were several *Thauera* strains isolated from various wastewater treatment systems (Liu *et al*., 2013). *Thauera* species are well known for their capability of degrading numerous aromatic compounds and terpenoids under denitrifying conditions, thereby contributing to their elimination from the environment.

Comparative genomic analyses (see Experimental procedures) indicated that this new genome and the genome of the type strain of T. *humireducens* shared an average nucleotide identity (ANI) of 98.16% and diverged by less than 0.5% in GC content. The overall difference in genome length was 326 kb with the genome presented here encoding 363 additional proteins. Taxonomic assignments performed using the Genome Taxonomy Database Toolkit [GTDB-Tk, (Chaumeil *et al*., 2020)] and DSMZ's Type Strain Genome Server platform [TYGS, (Meier-Kolthoff and Göker, 2019)] both indicated that the new genome is a new member of the T. *humireducens* species, first described in Yang *et al*. (2013).

Differential proteome analyses

To identify pivalate-induced genes in *T. humireducens*, the proteome of cells grown with pivalate/nitrate (in biological duplicate) were compared with cells grown with propionate/nitrate (biological triplicate) (For data sets see Table S3 provided as a supplementary data file). A volcano plot was performed to show the distribution of the proteomic data and the overall good reliability of the data obtained (Fig. S5).

We identified five different gene clusters containing genes displaying higher abundance in cells grown with pivalate versus propionate (log2 fold changes ≥2, Fig. 5). Cluster I comprises genes putatively encoding enzymes involved in pivalate activation to pivalyl-CoA and in the conversion of isovaleryl-CoA to acetoacetate and acetyl-CoA. Cluster V contains genes encoding the two subunits of an AdoCbl-dependent mutase, whereas cluster II harbours a pivalate-induced gene for a putative β-ketothiolase. Cluster III–V host genes for the conversion of precursors to the AdoCbl-cofactor of pivalyl-CoA mutase; in addition, genes for putative transporters of pivalate and AdoCbl precursors are present in two of the five clusters.

In summary, differential proteome analysis identified pivalate-induced gene products for almost all characteristic enzymatic reactions of the anaerobic pivalate degradation pathway that were measured by *in vitro* enzyme activities. Notably, AdoCbl-dependent mutases are involved in growth with both, pivalate and propionate,

Fig. 5. Differential proteome analysis of *T. humireducens* grown with pivalate versus propionate and assignment of gene products to the catabolic pivalate degradation pathway.
A. Gene clusters encoding proteins that are more abundant in cells grown with pivalate versus propionate. Genes that encode a putative AdoCbl-dependent pivalyl-CoA mutase are highlighted in red, those encoding two putative pivalate CoA ligases in green. Genes encoding other putative enzymes involved in pivalate degradation are depicted in blue; gene products involved in AdoCbl precursor utilization in pink, genes encoding a putative pivalate ABC transporter in ochre, and genes putatively involved in AdoCbl precursor transport in orange. The numbers shown above the genes refer to gene annotation in the genome of *T. humireducens* (C4PIVTH_v1_XXXX), and those shown below to the log2 fold changes in cells grown with pivalate versus propionate. UP = highly abundant proteins that were identified only in pivalate grown cells. Gene products marked with asterisks show *p*-values ≤0.05.
B. Annotation of pivalate-induced gene products to reactions of the pivalate degradation pathway. C4PIVTH_v1_0809 was heterologously expressed and its product was shown to act as a pivalate CoA ligase (Fig. 6).

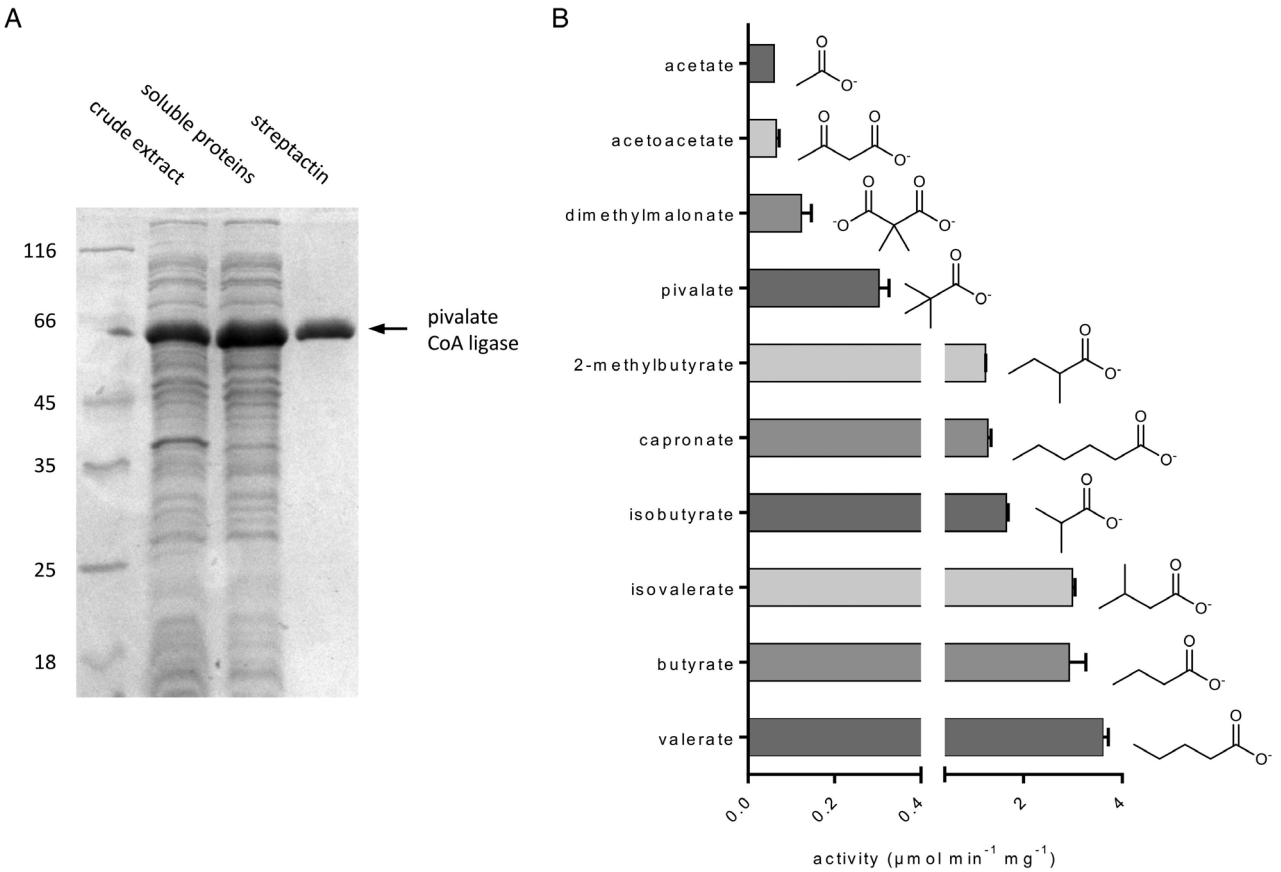

Fig. 6. Heterologous production and substrate preference of a carboxylic acid CoA ligase that accepts pivalate as substrate (C4PIVTH_v1_0809).
A. SDS gel of the enrichment of heterologously produced pivalate CoA ligase.
B. Substrate preference for selected carboxylic acids. The error bars refer to the standard deviation of three independent replicates.

acting on pivalyl-CoA and methylmalonyl-CoA respectively. The genome contains a gene cluster comprising genes encoding a putative methylmalonyl-CoA mutase and a propionyl-CoA carboxylase (Fig. S6) whose gene products together with a putative propionate CoA ligase were all less abundant in cells grown with pivalate versus propionate. Given that AdoCbl-dependent enzymes are required for pivalate and propionate catabolic pathways, the upregulation of cobalamin-utilizing genes in cells grown with pivalate versus propionate is unexpected. The low specific activity of pivalyl-CoA mutase compared to methylmalonyl-CoA mutase might be an explanation, as it is probably compensated by a significantly higher abundance in cells grown with pivalate, which in turn results in a higher demand for AdoCbl.

Heterologous production and characterization of a pivalyl-CoA forming ligase

Both, the C4PIVTH_v1_0809 and C4PIVTH_v1_3516 gene products show high amino acid sequence similarities to carboxylic acid CoA ligases from related Betaproteobacteria (up to 98.9% percentage identity), and a clearly higher abundance in cells grown with pivalate versus propionate. Furthermore, the encoding genes are located adjacent to other genes putatively involved in pivalate degradation or the putative pivalyl-CoA mutase (Fig. 5). For these reasons, we cloned and heterologously expressed both genes in *Escherichia coli* with a Strep-tag. With the C4PIVTH_v1_0809 gene product a soluble protein was formed, whereas C4PIVTH_v1_3516 was not produced at all with an N-terminal Strep-tag, or resulted in the formation of inactive inclusion bodies with a C-terminal Strep-tag (data not shown). The soluble gene product C4PIVTH_v1_0809 was highly enriched by Streptactin® affinity chromatography and eluted on SDS gels at the expected mass of around 65 kDa (Fig. 6A). The enzyme catalysed the MgATP-dependent formation of pivalyl-CoA from pivalate and CoA that followed Michaelis–Menten kinetics with apparent $K_m = 1.0 \pm 0.1$ mM and $V_{max} = 0.9 \pm 0.1$ µmol min^{-1} mg^{-1} (Fig. S7). The enzyme converted a number of aliphatic and branched carboxylic acids to their respective CoA esters and showed highest activity with C5

valerate (C5, Fig. 6B). Caproate (C6) was converted at a slightly lower rate, whereas capric acid (C10) was not converted. Small chain fatty acids such as acetate were activated only to a minor extent. Taken together, these results indicate that C4PIVTH_v1_0809, though not highly specific, acts as a pivalate CoA ligase during growth with pivalate. In addition, the pivalate-induced putative C4PIVTH_v1_3516 gene product may represent an additional pivalate activating enzyme.

Conclusion

In this work, we elucidated the previously unknown anaerobic degradation pathway of the quaternary carbon-containing model compound pivalate in the denitrifying *T. humireducens*. Data from *in vitro* enzyme activities, CoA ester metabolome, and proteogenomic analyses are fully consistent with a pathway that proceeds via CoA thioesterification to pivalyl-CoA followed by carbon skeleton rearrangement by an AdoCbl-dependent mutase. These two reactions are unique to this pathway, whereas the following reactions that convert isovaleryl-CoA to three acetyl-CoA units, including a carboxylation step, are shared with the leucine catabolic pathway. Compared with related enzymes, the *in vitro* activities of both reactions in cell extracts are rather low. The pivalyl-CoA mutase catalysed reaction represents the rate-limiting step of anaerobic pivalate degradation, which is reflected by the 1.5-fold higher doubling time during growth with pivalate versus propionate.

The AdoCbl-dependent strategy of the quaternary carbon skeleton rearrangement requires a CoA ester substrate to stabilize substrate and radical intermediates, similar as reported for methylmalonyl-CoA or butyryl-CoA mutases (Banerjee, 2003; Buckel *et al*., 2005). We propose that the anaerobic degradation of quaternary carbon-containing hydrocarbons such as isooctane might also follow such a strategy: (i) the anoxic oxidation of a methyl to carboxyl functionality, (ii) its thioesterification to a CoA thioester and (iii) rearrangement of the carbon skeleton by an AdoCbl-dependent mutase. The oxygen-independent oxidation of an unactivated methyl to a carboxylic acid functionality may proceed via addition to fumarate (Wilkes *et al*., 2016) or via alkyl coenzyme M intermediates (Zhou *et al*., 2022).

Experimental procedures

Chemicals and bacterial strains

The chemicals used in this work were of analytic grade and were obtained from Fluka (Neu-Ulm, Germany), Roth (Karlsruhe, Germany), AppliChem (Darmstadt, Germany), Sigma-Aldrich (Deisendorf, Germany), Gerbu (Heidelberg, Germany), Merck (Darmstadt, Germany), Becton Dickinson Company (Sparks, USA) and Grüssing (Filsum, Germany). *Thauera humireducens* strain PIV-1 (previously *Thauera pivalivorans* strain PIV1, DSMZ 14691) was obtained from the Deutsche Sammlung für Mikroorganismen und Zellkulturen (DSMZ).

Synthesis of CoA ester intermediates from free acids

Pivalyl-CoA and isovaleryl-CoA were synthesized from the corresponding free acids via a modified protocol as previously described (Willistein *et al*., 2018). For this purpose, 146.4 μmol of the corresponding free acid and equal amounts of tetramethyluronium tetrafluoroborate and 1-hydroxybenzotriazole hydrate were dissolved in 2 ml of dimethylformamide. 660 μmol of N,N-diisopropylethylamine was added and the mixture was incubated at room temperature for 10 min. Then 48.8 μmol of Li_3CoA dissolved in 200 μl of 0.1 M $NaHCO_3$ buffer (pH 8.3) was added and the mixture was stirred at room temperature for 30 min. The mixture was transferred to 10 ml of 20 mM sodium phosphate buffer (pH 6.8), filtered with 0.2 μM filters, and purified by preparative HPLC using an Atlantis® T3 Prep OBD™ column (5 μm, 19 × 250 mm). An acetonitrile/aqueous potassium phosphate buffer (10 mM, pH 6.8) gradient from 2% to 42% within 32 min was used for separation. The purified samples were evaporated, and lyophilized. The concentration of the synthesized CoA esters was determined using the Ellman's reagent. For this purpose, 50 μl of the synthesized CoA ester was hydrolyzed with 12.5 μl 4 M KOH at 25°C for 5 min. 25 μl of the mixture was transferred to 500 μl of potassium phosphate buffer (100 mM, pH 7.0) and 500 μl of Ellman's reagent [10 mM 5,5′-dithiobis-2-nitrobenzoic acid in 100 mM potassium phosphate buffer (pH 7.0)]. The concentration of hydrolyzed CoA was measured at 412 nm using a CoA calibration curve (0–0.25 mM).

Culture conditions, substrate consumption and preparation of cell extracts

Thauera humireducens was cultured anaerobically (N_2/CO_2, 80%/20%) at 30°C in mineral salt medium (0.5 g L^{-1} $MgSO_4 \times 7\ H_2O$, 0.5 g L^{-1} NH_4Cl, 0.5 g L^{-1} KH_2PO_4, 0.1 g L^{-1} $CaCl_2$, at pH 7.2). Vitamins (VL-7), trace elements (SL-10), 50 mM $NaHCO_3$, 5 mM pivalate (pH 7.0 with NaOH) and 15 mM $NaNO_3$ were added. Growth was monitored using a UV/VIS spectrophotometer at 578 nm. Pivalate and $NaNO_3$ were added continuously once nitrate was no longer detectable. Cells were harvested in the late exponential phase and frozen in liquid nitrogen. Frozen cells were lysed in a French pressure cell at 800 psi with a lysis buffer [50 mM MOPS/KOH (pH 7.0)

and 0.1 mg DNase I]. For enzymatic assays, cell extracts were ultracentrifuged (150 000*g*, 1 h, 4°C) and then desalted with 50 mM MOPS/KOH (pH 7.0) using PD Mini Trap G-25 columns according to the manufacturer's instructions. The protein content of the extract was determined using the Bradford assay. To determine substrate consumption, 1 ml of bacterial culture was withdrawn at different time points and centrifuged (10 000*g*, 10 min, 4°C). The supernatant (200 µl) was precipitated with 3.3 µl HCl (5 M) and then centrifuged. The supernatant (140 µl) was neutralized with 5 µl KOH (1 M) and measured using a Dionex ICS-2100 ion chromatography system. Separation was performed using a Dionex IonPac™ AS11-HC RFIC™ analytical column (2 × 250 mm) with an aqueous KOH gradient from 5 to 15 mM within 12 min. Substrate concentration was determined using a calibration curve for pivalate.

Enzymatic assays

Pivalate CoA ligase: Either a UPLC-based enzymatic assay or a coupled photometric assay was used to measure CoA ligase activity. For the coupled photometric assay, the following substances were used: 100 mM Tris/HCl (pH 7.8), 5 mM $MgCl_2$, 1 mM ATP, 0.4 mM CoA, 0.5 mM NADH, 2 mM dithioerythritol, 1 mM phosphoenolpyruvate, 2 U myokinase, 2 U pyruvate dehydrogenase, 2 U lactate dehydrogenase, 0.5 mM pivalic acid (or other substrates) and 20 µg ml^{-1} enriched ligase. Enzyme activity was determined by coupling ATP hydrolysis with reduction of NADH to NAD^+ at 365 nm (ε_{365} = 3400 M^{-1} cm^{-1}). The assay was started by adding the appropriate substrate.

The following chemicals were used for the UPLC-based assay: 50 mM Tris/HCl (pH 7.8), 4 mM $MgCl_2$, 2 mM ATP, 2 mM CoA and 1 mM pivalic acid. The assay was started with 2 mg ml^{-1} of desalted soluble proteins. The assays were incubated on a block heater at 30°C and 500 rpm, and stopped at various time points by transferring 20 µl of the sample to 40 µl of methanol on ice. For detection of intermediates by UPLC, the mixture was centrifuged at 8000*g* (4°C, 15 min). 20 µl of the supernatant was transferred to 80 µl H_2O. After an additional centrifugation step (8000*g*, 10 min, 4°C), the supernatant was loaded onto an Acquity H-Class UPLC system (Waters). Separation was performed on an Acquity UPLC HSS T3 C18 column (1.8 µm, 2.1 × 100 mm) using a one-step gradient from 0% to 20% acetonitrile in aqueous ammonium acetate buffer (10 mM) at a flow rate of 0.3 ml min^{-1} at 40°C. The separation was carried out within 6 min. The intermediates were detected at 260 nm.

Conversion of pivalyl-CoA to isovaleryl-CoA: The conversion was performed under anaerobic conditions (N_2/H_2, 95%/5%). For this purpose, 50 mM Tris/HCl (pH 7.8) and 1 mM pivalyl-CoA were used in the assay. Enriched pivalate CoA ligase (0.4 mg ml^{-1}), 2 mM MgATP and 1 mM CoA were added to minimize pivalyl-CoA depletion caused by a thioesterase activity. The assay was started with 2 mg ml^{-1} of desalted cell extract and run on a block heater at 30°C and 500 rpm. Samples were stopped and analysed by UPLC as described above.

Inactivation of pivalyl-CoA mutase by light: Irradiations with polychromatic light were performed with an 8-W LED lamp placed at a distance of 20 cm over 1 ml quartz cuvettes in an anaerobic tent at 10°C. Illuminance was 8200 lx. After irradiations, the soluble protein fraction of *T. humireducens* was used directly for the enzymatic assays using 50 mM Tris/HCl (pH 7.8) and 0.2 mM pivalyl-CoA. Enriched pivalate CoA ligase was added as described above to minimize pivalyl-CoA depletion.

Conversion of isovaleryl-CoA to 3-methylcrotonyl-CoA: The conversion of isovaleryl-CoA to 3-methylcrotonyl-CoA was performed on a block heater at 30°C and 500 rpm. For this, 50 mM Tris/HCl (pH 7.8), 5 mM $K_3[Fe(CN)_6]$ and 1 mM isovaleryl-CoA were used in the preparation. The enzymatic assay was started with 2 mg ml^{-1} of desalted cell extract. Samples were stopped and analysed by UPLC as described above.

Transformation of 3-methylcrotonyl-CoA to subsequent intermediates: For the conversion of 3-methyl-crotonyl-CoA to downstream products, samples were incubated for 30 min on a block heater at 30°C and 500 rpm using the following mixture: 50 mM Tris/HCl (pH 7.8), 4 mM $MgCl_2$, 5 mM $K_3[Fe(CN)_6]$, 10 mM sodium bicarbonate, 1 mM isovaleryl-CoA and 2 mg ml^{-1} desalted cell extracts. After 30 min, the assay was started with 2 mM ATP. Samples were stopped and measured by UPLC as described above.

Acetoacetate CoA ligase: To detect the acetoacetyl-CoA ligase activity, a UPLC-based enzymatic assay was conducted using the following set up: 50 mM Tris/HCl (pH 7.8), 2 mM $MgCl_2$, 1 mM ATP, 1 mM CoA and 0.5 mM acetoacetic acid. The assay was started with 0.2 mg ml^{-1} of desalted cell extract. The enzymatic assays were incubated on a block heater at 30°C and 500 rpm. The assays were stopped and measured via UPLC as described above.

UPLC-ESI-QTOF-MS analyses of CoA ester intermediates in whole cells

For extraction of metabolites, 45 ml of exponentially grown bacterial cultures (OD_{578} = 0.25–0.4) were centrifuged (20 min, 8000*g*, and 4°C). The precipitated cells were carefully mixed with 12 ml of 80% aqueous acetonitrile in 0.1 M formic acid and sonicated twice on ice for 30 s. Samples were frozen in liquid nitrogen and

lyophilized. The lyophilized samples were dissolved in 10 mM aqueous ammonium acetate, centrifuged twice at 10 000*g*, 10 min and 4°C, and analysed by UPLC-HRMS analyses. A Waters Acquity I-Class UPLC system with an Acquity UPLC HSS T3 C18 column (1.8 μm, 2.1 × 100 mm) coupled to a Waters Synapt G2-Si HRMS-ESI-QTOF-MS system was used to separate and detect pivalate-derived metabolites. A one-step gradient from 2% to 25% of acetonitrile and aqueous ammonium acetate (10 mM) was used within 35 min to separate the intermediates. The compounds were measured in positive mode with a capillary voltage of 3 kV, a source temperature of 150°C, a desolvation temperature of 450°C, an N_2 desolvation gas flow of 1000 L h^{-1} and an N_2 cone gas flow of 100 L h^{-1}.

UPLC-ESI-QTOF-MS analyses of pivalyl-CoA derived intermediates in assays with soluble cell extract

Samples were prepared as described for the UPLC-based enzymatic assays. An Acquity UPLC HSS T3 C18 column (1.8 μm, 2.1 × 100 mm) coupled to a Waters Synapt G2-Si HRMS-ESI-QTOF-MS system was used to separate and detect pivalate-derived metabolites. A one-step gradient from 0% to 20% acetonitrile (40°C) within 6 min in aqueous ammonium acetate buffer (10 mM) at a flow rate of 0.3 ml min^{-1} was used to separate the intermediates. The compounds were measured in positive mode with a capillary voltage of 2 kV, a source temperature of 100°C, a desolvation temperature of 500°C, an N_2 desolvation gas flow of 800 L h^{-1} and an N_2 cone gas flow of 30 L h^{-1}. Collision-induced dissociation of precursor ions was performed with a collision energy of 30 V. UPLC-HRMS data were analysed using MassLynx 4.1 (Waters). CoA esters were verified by detection of their characteristic fragment ions at *m/z* 428.0367, as described previously (Warnke *et al*., 2017).

Genome sequencing and annotation

Genome sequencing was performed using both short read (Illumina, San Diego, CA, USA) and long read (Oxford Nanopore Technologies, Oxford, UK, ONT) technologies.

For Illumina library preparation and sequencing, DNA (250 ng) was sonicated to a 100–1000 bp size range using the E220 Covaris Focused-ultrasonicator instrument (Covaris, Woburn, MA, USA). Fragments were end-repaired, then 3′-adenylated and NEXTflex HT Barcodes (Bioo Scientific, Austin, TX, USA) were added using NEBNext DNA modules products (New England Biolabs, Ipswich, MA, USA). After two consecutive clean ups with 1 × AMPure XP (Beckmann Coulter, Brea, CA, USA), the ligated product was amplified by 12 PCR cycles using the Kapa Hifi Hotstart NGS library amplification kit (KapaBiosystems, Wilmington, MA, USA), followed by purification with 0.8× AMPure XP (Beckmann Coulter). After library-profile analysis conducted with an Agilent 2100 Bioanalyzer (Agilent Technologies, Santa Clara, CA, USA) and qPCR quantification using the KAPA Library Quantification Kit for Illumina Libraries (KapaBiosystems), the library was sequenced with an Illumina MiSeq instrument using a 250 base-length read chemistry in a paired-end mode.

For ONT sequencing, the library was prepared according to Oxford Nanopore's 1D Native barcoding genomic DNA protocol (EXP-NBD104 and SQK-LSK109): genomic DNA fragments (1.5 μg) were repaired and 3′-adenylated with the NEBNext FFPE DNA Repair Mix and the NEBNext® Ultra™ II End Repair/dA-Tailing Module (New England Biolabs). Adapters with barcode provided by Oxford Nanopore Technologies were then ligated using the NEB Blunt/TA Ligase Master Mix (New England Biolabs). After purification with AMPure XP beads (Beckmann Coulter), two samples were pooled and sequencing adapters (ONT) were added using NEBNext Quick T4 DNA ligase (New England Biolabs). The final library was purified with AMPure XP beads (Beckmann Coulter), mixed with the Sequencing Buffer (ONT) and the Loading Bead (ONT), and loaded on a MinION R9.4.1 flow cell. Reads were basecalled using Guppy 2.3.5.

Sequences underwent standard in-house quality-check procedures, and were assembled using the SPAdes assembly engine (version 3.13.0) (Antipov *et al*., 2016) using the paired-end and nanopore libraries jointly. Both the main chromosome and plasmid sequences were uploaded into Genoscope's Microscope platform (Vallenet *et al*., 2020) for annotation, genome neighbourhood and comparative genomics analyses, and human curation.

Within the Microscope platform, the taxonomic assignment of the new genome was performed using the Genome Taxonomy DataBase Toolkit (Chaumeil *et al*., 2020) on the basis of the topology of the genome tree and of ANI values (Jain *et al*., 2018). In this pipeline, the Bacteria reference tree is inferred with FastTree (Price *et al*., 2010) under the WAG model from the concatenated alignment of 120 ubiquitous bacterial genes (Parks *et al*., 2018). An independent whole genome-based taxonomic assignment was also performed using the Type Strain Genome Database (TYGS, Meier-Kolthoff and Göker, 2019). Briefly, the taxonomic assignment was based on so-called 'digital DNA-DNA hybridization' (dDDH) values, computed according to the GBDP method (Meier-Kolthoff and Göker, 2019) between our genome and the 10 most closely related genomes (Table S4, provided as supplementary data file) initially

identified by MASH sketching (Ondov *et al*., 2016) of the TYGS type-strain genomes and refined using the GBDP approach (Meier-Kolthoff *et al*., 2013). The 16S SSU rDNA and genome trees of these genomes were not congruent, but a type-based species and subspecies clustering based on dDDH similarity values (Meier-Kolthoff and Göker, 2019) also indicated that our organism belongs to the Thauera *humireducens* species, the type strain of which was first described in Yang *et al*. (2013).

Proteome analyses

For protein analysis, samples were dissolved in 500 µl SDS lysis buffer (0.29 g NaCl, 1 M Tris/HCL pH 8.0, 5 M EDTA pH 8.0, 0.4 g SDS in 100 ml water). Protein extraction was done by disrupted via bead beating (FastPrep-24, MP Biomedicals, Santa Ana, CA, USA; 5.5 ms, 1 min, 3 cycles) followed by ultra-sonication (UP50H, Hielscher, Teltow, Germany; cycle 0.5, amplitude 60%) and centrifugation (10 000*g*, 10 min). The protein lysate was loaded on SDS-gel and run for 10 min. The gel piece was cut, washed and incubated with 25 mM 1,4 dithiothreitol (in 20 mM ammonium bicarbonate) for 1 h and 100 mM iodoacetamide (in 20 mM ammonium bicarbonate) for 30 min, and destained, dehydrated and proteolytically cleaved overnight at 37°C with trypsin (Promega). The digested peptides were extracted and desalted using ZipTip µC18 tips (Merck Millipore, Darmstadt, Germany). The peptide lysates were re-suspended in 15 µl 0.1% formic acid and analysed by nanoliquid chromatography mass spectrometry (UltiMate 3000 RSLCnano, Dionex, Thermo Fisher Scientific). Mass spectrometric analyses of eluted peptide lysates were performed on a Q Exactive HF mass spectrometer (Thermo Fisher Scientific) coupled with a TriVersa NanoMate (Advion, Harlow, UK). Peptide lysates were injected on a trapping column (Acclaim PepMap 100 C18, 3 µm, nanoViper, 75 µm × 2 cm, Thermo Fisher Scientific) with 5 µl min^{-1} by using 98% water/2% ACN 0.5% trifluoroacetic acid, and separated on an analytical column (Acclaim PepMap 100 C18, 3 µm, nanoViper, 75 µm × 25 cm, Thermo Fisher Scientific) with a flow rate of 300 nl min^{-1}. Mobile phase was 0.1% formic acid in water (A) and 80% ACN/0.08% formic acid in water (B). Full MS spectra (350–1550 *m/z*) were acquired in the Orbitrap at a resolution of 120 000 with automatic gain control (AGC) target value of 3×10^6 ions.

Data resulting from LC–MS/MS measurements were analysed with the Proteome Discoverer (v.2.4, Thermo Fischer Scientific) using SEQUEST HT. Protein identification was performed using a self-built reference database downloaded from UniProt (*Thauera humireducens PIV1*). Searches were conducted with the following parameters: Trypsin as enzyme specificity and two missed cleavages allowed. A peptide ion tolerance of 10 ppm and an MS/MS tolerance of 0.02 Da were used. As modifications, oxidation (methionine) and carbamidomethylation (cysteine) were selected. Peptides that scored a *q*-value >1% based on a decoy database and with a peptide rank of 1 were considered identified.

Heterologous gene expression, production and enrichment of recombinant pivalate CoA ligase in E. coli *BL21*

The gene encoding pivalate CoA ligase (C4PIVTH_v1_0809) was amplified with an N-terminal strep tag by PCR from genomic DNA of T. *humireducens* using the following primers: 0809_for (GTACGTGAATTCAGCA GTACGCAGAGCTATGTC) and 0809_rev (TGACTGAAGC TTTCGATGTCAGGCGGTCTG). The resulting 1.7 kb PCR fragment was double digested with HindIII/EcoRI, cloned into pASK-IBA15plus, and transformed into *E. coli* NEB 5α according to New England Biolabs (NEB) protocols. The resulting plasmid was isolated and transformed into *E. coli* BL21 according to NEB protocols. Pivalate CoA ligase was induced in 2× YT medium (18 g L^{-1} tryptone, 10 g L^{-1} yeast extracts and 5 g L^{-1} NaCl) supplemented with 100 µg ml^{-1} ampicillin. Anhydrotetracycline (20 µg ml^{-1}) was added after the cells reached an optical density of 0.6. Induction was performed at 20°C and 180 rpm. Cells were harvested in the late exponential phase by centrifugation (8000*g*, 20 min, and 4°C) and frozen in liquid nitrogen.

Crude extracts were prepared by dissolving cells in double the amount of lysis buffer [50 mM MOPS/KOH (pH 7.0) and 0.1 mg DNase I] and digested using a French pressure cell at 1100 psi. Soluble proteins were recovered by ultracentrifugation (150 000*g*, 1 h and 4°C). The soluble protein fraction was applied to a Strep-Tactin affinity column (12 ml, Cytiva) at 2 ml min^{-1}. The column was equilibrated with buffer A (50 mM HEPES/KOH pH 7.6, 150 mM KCl). The active protein fraction was eluted with buffer B (50 mM HEPES/KOH pH 7.6, 150 mM KCl and 5 mM desthiobiotin). The enriched protein was concentrated (10-kDa cut-off membrane), desalted (PD-10 column) and stored at −20°C (20.1 mg ml^{-1}) or −80°C for long-term storage.

Acknowledgements

This work was funded by the Germany Research Council (DFG) project number 235777276. T.B. thanks Genoscope's LABGeM team for running the MicroScope genome annotation platform, and Corinne Cruaud and Genoscope's sequencing team for assistance with genome sequencing.

Data Availability

Genome data have been deposited at ENA/NCBI/DDBJ databases under accession numbers OW011623 and OW011624 (study identifier PRJEB51144). Data sets of proteome analyses are available in the Supporting Information. All other data of this study are available from the corresponding author upon reasonable request.

References

Antipov, D., Korobeynikov, A., McLean, J.S., and Pevzner, p.A. (2016) hybridSPAdes: an algorithm for hybrid assembly of short and long reads. *Bioinformatics* **32**: 1009–1015.

Banerjee, R. (2003) Radical carbon skeleton rearrangements: catalysis by coenzyme B12-dependent mutases. *Chem Rev* **103**: 2083–2094.

Bisel, P., Al-Momani, L., and Müller, M. (2008) The tert-butyl group in chemistry and biology. *Org Biomol Chem* **6**: 2655–2665.

Brass, E.P. (2002) Pivalate-generating prodrugs and carnitine homeostasis in man. *Pharmacol Rev* **54**: 589–598.

Buckel, W., Kratky, C., and Golding, B.T. (2005) Stabilisation of methylene radicals by cob(II)alamin in coenzyme B12 dependent mutases. *Chemistry* **12**: 352–362.

Chaumeil, p.A., Mussig, A.J., Hugenholtz, P., and Parks, D. H. (2020) GTDB-Tk: a toolkit to classify genomes with the Genome Taxonomy Database. *Bioinformatics* **36**: 1925–1927.

Chohnan, S., and Takamura, Y. (2004) Minireview malonate decarboxylase in bacteria and its application for determination of intracellular acyl-CoA thioesters. *Microbes Environ* **19**: 179–189.

Dembitsky, V.M. (2006) Natural neo acids and neo alkanes: their analogs and derivatives. *Lipids* **41**: 309–340.

Dermer, J., and Fuchs, G. (2012) Molybdoenzyme that catalyzes the anaerobic hydroxylation of a tertiary carbon atom in the side chain of cholesterol. *J Biol Chem* **287**: 36905–36916.

Franz, L., Kazmaier, U., Truman, A.W., and Koehnke, J. (2021) Bottromycins – biosynthesis, synthesis and activity. *Nat Prod Rep* **38**: 1659–1683.

Jacoby, C., Goerke, M., Bezold, D., Jessen, H., and Boll, M. (2021). A fully reversible 25-hydroxy steroid kinase involved in oxygen-independent cholesterol side-chain oxidation. *J Biol Chem* **297**: 101105.

Jacoby, C., Eipper, J., Warnke, M., Tiedt, O., Mergelsberg, M., Stärk, H.-J., *et al*. (2018) Four molybdenum-dependent steroid C-25 hydroxylases: heterologous overproduction, role in steroid degradation, and application for 25-hydroxyvitamin D 3 synthesis. *MBio* **9**: e00694-18.

Jacoby, C., Ferlaino, S., Bezold, D., Jessen, H., Müller, M., and Boll, M. (2020a) ATP-dependent hydroxylation of an unactivated primary carbon with water. *Nat Commun* **11**: 3906.

Jacoby, C., Krull, J., Andexer, J., Jehmlich, N., von Bergen, M., Brüls, T., and Boll, M. (2020b) Channeling c1 metabolism toward s-adenosylmethionine-dependent conversion of estrogens to androgens in estrogen-degrading bacteria. *MBio* **11**: 1–16.

Jain, C., Rodriguez-R, L.M., Phillippy, A.M., Konstantinidis, K. T., and Aluru, S. (2018) High throughput ANI analysis of 90K prokaryotic genomes reveals clear species boundaries. *Nat Commun* **91**: 1–8.

Jarling, R., Sadeghi, M., Drozdowska, M., Lahme, S., Buckel, W., Rabus, R., *et al*. (2012) Stereochemical investigations reveal the mechanism of the bacterial activation of n-alkanes without oxygen. *Angew Chem Int Ed Engl* **51**: 1334–1338.

Kenig, F., Simons, D.J.H., Crich, D., Cowen, J.P., Ventura, G.T., Rehbein-Khalily, T., *et al*. (2003) Branched aliphatic alkanes with quaternary substituted carbon atoms in modern and ancient geologic samples. *Proc Natl Acad Sci* **100**: 12554–12558.

Kitanishi, K., Cracan, V., and Banerjee, R. (2015) Engineered and native coenzyme B12-dependent isovaleryl-CoA/pivalyl-CoA mutase. *J Biol Chem* **290**: 20466–20476.

Kniemeyer, O., Probian, C., Rosselló-Mora, R., and Harder, J. (1999) Anaerobic mineralization of quaternary carbon atoms: isolation of denitrifying bacteria on dimethylmalonate. *Appl Environ Microbiol* **65**: 3319–3324.

Liu, B., Frostegård, Å., and Shapleigh, J.P. (2013) Draft genome sequences of five strains in the genus *Thauera*. *Genome Announc* **1**: e00052-12.

Marmulla, R., and Harder, J. (2014) Microbial monoterpene transformations – a review. *Front Microbiol* **5**: 346.

Massey, L.K., Sokatch, J.R., and Conrad, R.S. (1976) Branched-chain amino acid catabolism in bacteria. *Bacteriol Rev* **40**: 42–54.

Meier-Kolthoff, J.P., Auch, A.F., Klenk, H.P., and Göker, M. (2013) Genome sequence-based species delimitation with confidence intervals and improved distance functions. *BMC Bioinformatics* **14**: 1–14.

Meier-Kolthoff, J.P., and Göker, M. (2019) TYGS is an automated high-throughput platform for state-of-the-art genome-based taxonomy. *Nat Commun* **101**: 1–10.

Nemecek-Marshall, M., Wojciechowski, C., Wagner, W.P., and Fall, R. (1999) Acetone formation in the vibrio family: a new pathway for bacterial leucine catabolism. *J Bacteriol* **181**: 7493–7499.

Ondov, B.D., Treangen, T.J., Melsted, P., Mallonee, A.B., Bergman, N.H., Koren, S., and Phillippy, A.M. (2016) Mash: fast genome and metagenome distance estimation using MinHash. *Genome Biol* **17**: 1–14.

Parks, D.H., Chuvochina, M., Waite, D.W., Rinke, C., Skarshewski, A., Chaumeil, p.A., and Hugenholtz, P. (2018) A standardized bacterial taxonomy based on genome phylogeny substantially revises the tree of life. *Nat Biotechnol* **3610**: 996–1004.

Price, M.N., Dehal, p.S., and Arkin, A.P. (2010) FastTree 2 – approximately maximum-likelihood trees for large alignments. *PLoS One* **5**: e9490.

Probian, C., Wülfing, A., and Harder, J. (2003) Anaerobic mineralization of quaternary carbon atoms: isolation of denitrifying bacteria on pivalic acid (2,2-dimethylpropionic acid). *Appl Environ Microbiol* **69**: 1866–1870.

Shyadehi, A.Z., Lamb, D.C., Kelly, S.L., Kelly, D.E., Schunck, W.H., Wright, J.N., *et al*. (1996) The mechanism

of the acyl-carbon bond cleavage reaction catalyzed by recombinant sterol 14α-demethylase of Candida albicans (other names are: lanosterol 14α-demethylase, P-45014DM, and CYP51). *J Biol Chem* **271**: 12445–12450.
Simpson, E.R., Clyne, C., Rubin, G., Boon, W.C., Robertson, K., Britt, K., *et al*. (2002) Aromatase—a brief overview. *Annu Rev Physiol* **64**: 93–127.
Solano-Serena, F., Marchal, R., Casarégola, S., Vasnier, C., Lebeault, J.M., and Vandecasteele, J.P. (2000) A Mycobacterium strain with extended capacities for degradation of gasoline hydrocarbons. *Appl Environ Microbiol* **66**: 2392–2399.
Solano-Serena, F., Marchal, R., Heiss, S., and Vandecasteele, J.P. (2004) Degradation of isooctane by Mycobacterium austroafricanum IFP 2173: growth and catabolic pathway. *J Appl Microbiol* **97**: 629–639.
Trudgill, p.W. (1994) Microbial metabolism and transformation of selected monoterpenes. *Biochemistry of microbial degradation*: 33–61.
Vallenet, D., Calteau, A., Dubois, M., Amours, P., Bazin, A., Beuvin, M., *et al*. (2020) MicroScope: an integrated platform for the annotation and exploration of microbial gene functions through genomic, pangenomic and metabolic comparative analysis. *Nucleic Acids Res* **48**: 579–589.
Wang, P.-H., Chen, Y.-L., Wei, S.T.-S., Wu, K., Lee, T.-H., Wu, T.-Y., and Chiang, Y.-R. (2020) Retroconversion of estrogens into androgens by bacteria via a cobalamin-mediated methylation. *Proc Natl Acad Sci* **117**: 1395–1403.
Wang, P.-H., Lee, T.-H., Ismail, W., Tsai, C.-Y., Lin, C.-W., Tsai, Y.-W., and Chiang, Y.-R. (2013). An oxygenase-independent cholesterol catabolic pathway operates under Oxic Conditions. *PLoS ONE* **8**: e66675.
Warnke, M., Jacoby, C., Jung, T., Agne, M., Mergelsberg, M., Starke, R., *et al*. (2017) A patchwork pathway for oxygenase-independent degradation of side chain containing steroids. *Environ Microbiol* **19**: 4684–4699.
Wilkes, H., Buckel, W., Golding, B.T., and Rabus, R. (2016) Metabolism of hydrocarbons in n-alkane-utilizing anaerobic bacteria. *J Mol Microbiol Biotechnol* **26**: 138–151.
Willistein, M., Haas, J., Fuchs, J., Estelmann, S., Ferlaino, S., Müller, M., *et al*. (2018) Enantioselective enzymatic naphthoyl ring reduction. *Chemistry* **24**: 12505–12508.
Yang, G.Q., Zhang, J., Kwon, S.W., Zhou, S.G., Han, L.C., Chen, M., *et al*. (2013) *Thauera humireducens* sp. nov., a humus-reducing bacterium isolated from a microbial fuel cell. *Int J Syst Evol Microbiol* **63**: 873–878.
Zhou, Z., Zhang, C.-J., Liu, P.-F., Fu, L., Laso-Pérez, R., Yang, L., *et al*. (2022) Non-syntrophic methanogenic hydrocarbon degradation by an archaeal species. *Nature* **601**: 257–262.

Supporting Information

Additional Supporting Information may be found in the online version of this article at the publisher's web-site:

Fig. S1. Time-dependent inactivation of putative pivalyl-CoA mutase activity with polychromatic light. *A*. In the presence of polychromatic light, the conversion of pivalyl-CoA to isovaleryl-CoA was time-dependently inhibited. *B*. Reactivation of the activity after irradiation with polychromatic light (120 min) by addition of 20 μM AdoCbl. The error bars refer to the standard deviation of three independent replicates.

Fig. S2. Leucine catabolic pathway via 3-methylcro tonyl-CoA.

Fig. S3. Time-dependent conversion of acetoacetate to two acetyl-CoA. In the presence of MgATP and CoA, acetoacetate was activated to acetoacetyl-CoA that is rapidly cleaved to two acetyl-CoA (**7**) by β-ketothiolase. The UPLC-based enzymatic assays contained 0.2 mg ml^{-1} proteins, samples were taken at 0, 1, 2, 5 and 15 min. The numbers refer to components identified by ESI-Q-TOF-MS/MS analyses listed in Table S2, and to metabolites depicted in Fig. 5.

Fig S4. Main chromosome of *Thauera humireducens* strain PIV-1. This figure was produced using the Proksee web server (https://proksee.ca/).

Fig. S5. Volcano-plot of overall proteomic data (see Table S3/supplementary data file: Proteome data *Thauera humireducens* strain PIV-1.xls) with cells grown with pivalate/nitrate (in biological duplicate) to cells grown with propionate/nitrate (biological triplicate). Measurements in which no signal was detectable in one or more samples are grayed out. UP: highly abundant proteins in cells grown with pivalate/nitrate, DOWN: highly abundant proteins in cells grown with propionate/nitrate.

Fig. S6. Abundance of gene products putatively involved in propionate degradation in *T. humireducens* strain PIV-1 cells grown on pivalate versus propionate. The numbers shown above the genes refer to gene annotation in the genome of *T. humireducens* (C4PIVTH_v1_XXXX), and numbers shown below to the log2 fold changes in cells grown with pivalate versus propionate.

Fig. S7. Dependence of pivalate CoA ligase activity on the substrate concentrations. The data points were fitted to a Michaelis–Menten curve with $K_m = 1.0 \pm 0.1$ mM and $V_{max} = 0.9 \pm 0.1$ μmol min^{-1} mg^{-1}. The error bars refer to the standard deviation of three independent replicates.

Table S1. UPLC-ESI-QTOF-MS analyses of selected CoA-ester intermediates in whole *T. humireducens* strain PIV-1 cells. The calculated and measured *m/z* values, mass deviations (ΔmDa) and retention times (R_t) are given.

Table S2. UPLC-ESI-QTOF-MS/MS analyses of pivalyl-CoA and pivalyl-CoA-derived intermediates identified in in vitro assays with soluble extracts from *T. humireducens* strain PIV-1. The calculated and measured *m/z* values, mass deviations (ΔmDa) and retention times (R_t) for the parent and daughter ion peaks are given.

Table S3. Data sets of proteome analyses of *T. humireducens* strain PIV-1 grown on pivalate/nitrate (Data records S1–S2) and propionate/nitrate (Data records S3–S5); see supplementary data file: Proteome data *Thauera humireducens* strain PIV-1 proteome data.xls.

Table S4. Compilation of genomes from *Thauera* type strains with the genome of the *Thauera* strain PIV1 (C4PIVTH.1) investigated in this work; see supplementary data file: Close type strain genomes.xls.

Appendix S1. Supporting Information.